



# Soft Tissue Stabilization of the Hinge Position for Lateral Closing-Wedge Distal Femoral Osteotomy

## An Anatomic Study

Taiga Oda,\* MD, Akira Maeyama,\*<sup>†</sup> MD, PhD, Tetsuro Ishimatsu,\* MD, PhD, Katsuro Tachibana,<sup>‡</sup> MD, PhD, Kengo Yoshimitsu,<sup>§</sup> MD, PhD, and Takuaki Yamamoto,\* MD, PhD  
Investigation performed at Fukuoka University Faculty of Medicine, Fukuoka, Japan

**Background:** Soft tissue plays an important role in stabilizing the hinge point for osteotomy around the knee. However, insufficient data are available on the anatomic features of the soft tissue around the hinge position for lateral closing-wedge distal femoral osteotomy (LCWDFO).

**Purpose:** To (1) anatomically analyze the soft tissue around the hinge position for LCWDFO, (2) histologically analyze the soft tissue based on the anatomic analysis results, and (3) radiologically define the appropriate hinge point to prevent unstable hinge fracture based on the results of the anatomic and histological analyses.

**Study Design:** Descriptive laboratory study.

**Methods:** In 20 cadaveric knees (age,  $82.7 \pm 7.8$  years; range, 60-96 years), the soft tissue of the distal medial side of the femur was anatomically analyzed. The thicknesses of the periosteum and direct insertion of the adductor tendon (AT) were histologically examined and measured using an electron microscope. The thickness of the periosteum was visualized graphically, and the graph of the periosteum and radiograph of the knee were overlaid using image editing software. The appropriate hinge position was determined based on the periosteal thickness and attachment of the AT.

**Results:** The mean thickness of the periosteum of the metaphysis was  $352.7 \pm 58.6 \mu\text{m}$  (range, 213.6-503.4  $\mu\text{m}$ ). The overlaid graph and radiograph revealed that the thickness of the periosteum changed at the part corresponding to the transition between the diaphyseal and metaphyseal ends of the femur. The mean width of the AT attached to the distal medial femur from the adductor tubercle toward the distal direction was  $7.9 \pm 1.3 \text{ mm}$  (range, 6.3-9.7 mm).

**Conclusion:** Results indicated that the periosteum and AT support the hinge for LCWDFO within the area surrounded by the apex of the adductor tubercle and the upper border of the posterior part of the lateral femoral condyle.

**Clinical Relevance:** When the hinge point is located within the area surrounded by the apex of the adductor tubercle and the upper border of the posterior part of the lateral femoral condyle, these soft tissues work as stabilizers, and there is no risk of cutting into the joint space.

**Keywords:** lateral closing-wedge distal femoral osteotomy; hinge point; periosteum; adductor tendon; attachment

Medial opening-wedge high tibial osteotomy (MOWHTO) is an established treatment to correct varus knee in young, active patients.<sup>11,23</sup> However, single-level osteotomy for knees with severe varus deformity requires a large amount of correction, which forms nonanatomic joint line obliquity

and results in poor clinical outcomes.<sup>1,16,22</sup> To avoid these unfavorable outcomes, double-level osteotomy that combines MOWHTO with lateral closing-wedge distal femoral osteotomy (LCWDFO) has been recommended to avoid excessive joint line obliquity.<sup>2,21</sup>

The reported survival rate of double-level osteotomy is 96% at 10 years postoperatively, and an acceptable clinical outcome is expected once the osteotomy site is united.<sup>2,21</sup> However, unstable medial hinge fracture is considered an

The Orthopaedic Journal of Sports Medicine, 12(3), 23259671241233014  
DOI: 10.1177/23259671241233014  
© The Author(s) 2024

This open-access article is published and distributed under the Creative Commons Attribution - NonCommercial - No Derivatives License (<https://creativecommons.org/licenses/by-nc-nd/4.0/>), which permits the noncommercial use, distribution, and reproduction of the article in any medium, provided the original author and source are credited. You may not alter, transform, or build upon this article without the permission of the Author(s). For article reuse guidelines, please visit SAGE's website at <http://www.sagepub.com/journals-permissions>.

important cause of instability at the distal femoral osteotomy site, which may lead to displacement at the osteotomy site, malunion or nonunion, and loss of correction.<sup>8,13,20</sup> Therefore, several studies have attempted to define the “safe zone” for intracapsular–extra-articular osteotomy around the knee in which the risk of unstable hinge fracture is minimized and there is no risk of cutting into the joint space in the distal direction.<sup>6,14,15,18</sup>

The local soft tissue reportedly plays an important role in stabilizing the hinge point of osteotomy around the knee. In MOWHTO, the joint capsule–periosteal sleeve and the tibialis anterior muscle work as soft tissue stabilizers in the region from the tip of the fibular head to the circumference line of the fibular head, and this area has been termed the “safe zone.”<sup>6,15</sup> Furthermore, we have previously reported that the periosteum supports the hinge of medial closing-wedge distal femoral osteotomy (MCWDFO) within the area surrounded by the apex of the turning point of the femoral metaphysis and the upper border of the posterior part of the lateral femoral condyle.<sup>18</sup>

In addition to these soft tissues, the tendon attachments act as an anchor that is expected to stabilize the hinge point. The enthesis of the tendon is classified into 2 categories depending on the presence or absence of a fibrocartilaginous layer and is expressed as having “direct” or “indirect” insertion.<sup>5,9</sup> Direct insertion has a 4-layered structure consisting of a fibrous tissue layer, noncalcified fibrocartilage layer, calcified fibrocartilage layer, and bone layer. Direct insertion is thought to have stronger mechanical properties than indirect insertion in which the ligamentous tissue attaches to the bone tissue without the fibrocartilage layer.<sup>4</sup>

Although soft tissue is expected to play a role in stabilizing the hinge point for LCWDFO as well as in other osteotomies, no detailed studies of the soft tissue or safe zone for LCWDFO have been conducted. The purposes of the present study were to (1) anatomically analyze the soft tissue (including the periosteum and adductor tendon [AT] insertion) around the hinge point for LCWDFO, (2) histologically analyze the soft tissue based on the results of the anatomic analysis, and (3) radiologically define the appropriate hinge point to prevent unstable hinge fracture based on the results of the anatomic and histological analyses. We hypothesized that the safe zone of the hinge point for LCWDFO would be clarified by analyzing the soft tissue of the distal medial femur.

## METHODS

A total of 30 knees from 30 cadavers donated to our institute between July 2016 and April 2020 were considered

for this study. Five knees were excluded because of flexion contracture and severe osteoarthritis, whereas another 5 knees were reserved for the pilot studies. As a result, a total of 20 knees from 20 cadavers were used in the main analysis (10 men and 10 women; 10 right knees and 10 left knees; mean age at the time of death,  $82.7 \pm 7.8$  years [range, 60–96 years]; height,  $161.4 \pm 7.3$  cm [range, 150–178 cm]). The cadavers were fixed with 37% formalin and preserved in 95% ethanol. The protocol for the present study was approved by our institutional review board before study commencement.

## Anatomic Analysis of the Soft Tissue Around the Hinge Point for LCWDFO

Pilot tests were performed to investigate the soft tissue around the distal medial femur in 3 knees. A  $30 \times 30$ -cm piece of skin was excised from the distal medial side of the knee joint, and capsulotomy was performed via the medial parapatellar approach. The joint capsule was dissected while leaving the attachments and was inverted proximally with the vastus medialis and quadriceps muscles. Subsequently, the tendons of the sartorius, gracilis, and semitendinosus muscles were dissected from the tibia and inverted proximally. Finally, the mediolateral (ML) and anteroposterior (AP) dimensions of the femoral condyle and the total length of the femur were measured at 0.1-mm intervals using a digital caliper (IP54 digital caliper; Gawoow).

## Histological Examination of Soft Tissue

Soft tissue (bone, periosteum, and adductor muscle-tendon complex) was removed from the medial side of the distal femur starting from the medial epicondyle toward the proximal direction and histologically examined (Figure 1, A and C). For comparison, a 3 cm–wide section of soft tissue was also removed from the medial side of the femoral shaft (bone and periosteum complex) (Figure 1B).

The specimens were sliced with a pathology saw to produce a block comprising the femur and periosteum and another comprising the AT. The blocks were fixed in 8% formalin and decalcified in a solution containing aluminum chloride, hydrochloric acid, and formic acid, as reported previously.<sup>19</sup> The blocks were then embedded in paraffin and sliced into 5- $\mu$ m sections. Sections were stained with hematoxylin and eosin (HE) stain and Masson trichrome (MT) stain, as described previously.<sup>17,18</sup> The thickness of the stained periosteum and direct insertion of the AT

<sup>†</sup>Address correspondence to Akira Maeyama, MD, PhD, Department of Orthopedic Surgery, Fukuoka University Faculty of Medicine, 7-45-1 Nanakuma, Jonan-ku, Fukuoka, 814-0180, Japan (email: akira.maeyama0713@joy.ocn.ne.jp).

\*Department of Orthopedic Surgery, Fukuoka University Faculty of Medicine, Fukuoka, Japan.

<sup>‡</sup>Department of Anatomy, Fukuoka University Faculty of Medicine, Fukuoka, Japan.

<sup>§</sup>Department of Radiology, Fukuoka University Faculty of Medicine, Fukuoka, Japan.

Final revision submitted August 28, 2023; accepted September 6, 2023.

The authors have declared that there are no conflicts of interest in the authorship and publication of this contribution. AOSM checks author disclosures against the Open Payments Database (OPD). AOSM has not conducted an independent investigation on the OPD and disclaims any liability or responsibility relating thereto.

Ethical approval for this study was obtained from Fukuoka University Faculty of Medicine (ref No. U20-663).

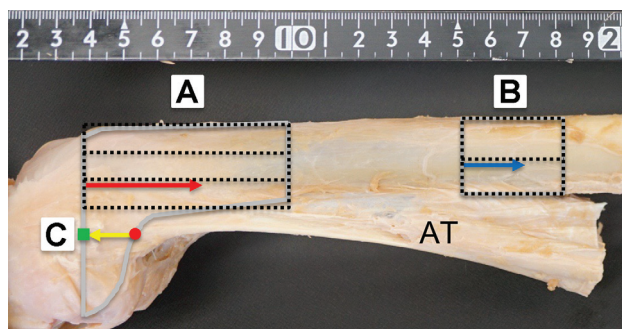


**Figure 1.** Histological section of the medial femur. (A) Metaphysis region: the histological section passes through two-thirds of the divided area where the hinge point for lateral closing-wedge distal femoral osteotomy is usually made (red arrow). (B) Diaphysis region: the histological section passes through the middle of the divided area (blue arrow). (C) Adductor tubercle region: the histological section is made to examine the attachment of the adductor tendon starting from the adductor tubercle (red dot) and parallel to the metaphysis section (yellow arrow). The green square is the medial epicondyle. AT, adductor tendon.

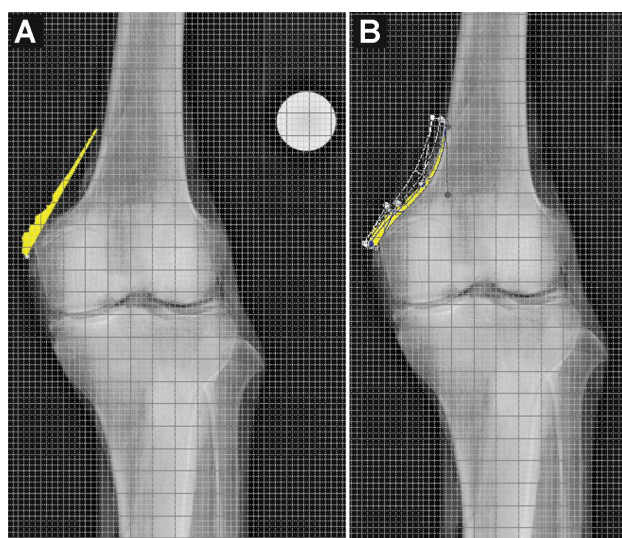


**Figure 2.** Radiograph overlaid with the graphed periosteal thickness (shaded in yellow). (A) Before deformation: the graph is calibrated to the radiograph with a 2.5-cm calibrator (white circle). (B) After deformation: the graph is deformed along the curved part of the metaphysis of the distal femur using a previously reported method.<sup>18</sup>

were measured using an electron microscope (Olympus BX50) at intervals of 500  $\mu$ m. The electron microscope images were recorded with a microscope camera (Olympus DP27-B). The results of the measured periosteal thickness were visualized graphically using Excel (Version 16.81; Microsoft Corp).

TABLE 1

Cadaveric Characteristics and Femoral Measurements<sup>a</sup>

Variable	Value
Side, right/left	10/10
Sex, male/female	10/10
Age, y	82.7 $\pm$ 7.8 (60-96)
Height, cm	161.4 $\pm$ 7.3 (150-178)
Mediolateral dimension of distal femur, mm	83.7 $\pm$ 5.7 (74.0-93.3)
Anteroposterior dimension of distal femur, mm	66.0 $\pm$ 6.2 (54.2-76.0)
Length of femur, cm	42.4 $\pm$ 4.1 (37.0-48.0)

<sup>a</sup>Data are reported as n or mean  $\pm$  SD (range).

### Radiological Analysis of Periosteal Thickness

Frontal and lateral radiographs of all amputated knees were taken with a 2.5-cm calibrator under the following radiographic conditions: 70 kV, 7 mAs, and distance of 120 cm. Using a method reported in a previous study,<sup>18</sup> we overlaid the graphical representation of the periosteal thickness on a frontal radiograph of the knee using image editing software (Adobe Photoshop Version cs6) (Figure 2).

### Statistical Analysis

All statistical analyses were performed using SPSS Version 23.0 software (IBM). All continuous variables were described as mean  $\pm$  standard deviation. Pearson correlation analysis was used to analyze the association of cadaveric characteristics and distal femoral dimensions with (1) periosteal thickness at the metaphysis and diaphysis and (2) direct insertion of the AT. For all statistical comparisons, *P* values  $<$ .05 were considered significant.

## RESULTS

### Anatomy of the Medial Side of the Distal Femur

Our pilot study revealed the presence of the joint capsule, AT, and periosteum on the medial side of the distal femur (Figure 3).

Quantitative measurements of the femur revealed that the mean ML dimension was 83.7  $\pm$  5.7 mm (range, 74.0-93.3 mm), mean AP dimension was 66.0  $\pm$  6.2 mm (range, 54.2-76.0 mm), and mean total length of the femur was 42.4  $\pm$  4.1 cm (range, 37.0-48.0 cm). The cadaveric characteristics and measured femoral widths and lengths are shown in Table 1.

### Histological Examination of Soft Tissue

The histological findings of the distal medial femur are shown in Figure 4. A continuous layered structure on the

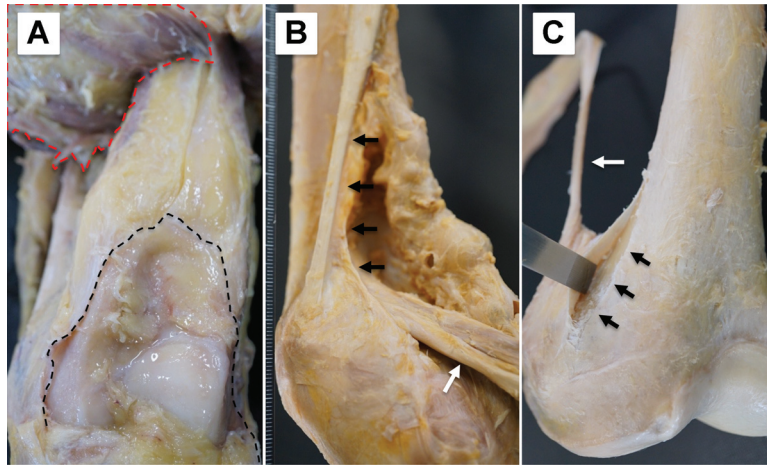


**Figure 3.** Soft tissue on the distal medial aspect of the femur. (A) Frontal view of the femur in a left knee. The capsule of the suprapatellar bursa is separated at the femoral attachment (black dashed line), and the vastus medialis and quadriceps muscles are inverted proximally (red dashed line). (B) Lateral view of the femur in a right knee. The adductor muscle tendon (AT) is attached distally to the femur in a fan shape (black arrows), and the medial head of the gastrocnemius muscle is attached to the posterior aspect of the femur (white arrow). (C) Lateral view of the femur in a left knee. The periosteum of the metaphysis is detached by a rasper (black arrows); the white arrow indicates the AT.

bone cortex was observed in the low-powered HE-stained image (Figure 4B). The high-powered HE-stained image showed 2 layers: the cambium layer directly adjacent to the outer surface of the bone cortex and the outer fibrous layer (Figure 4C). These layered structures were deeply and equally stained blue by MT and gradually thinned from the distal to the proximal direction. Thus, these layers were considered to be the periosteum (Figure 4D). The measured mean periosteal thicknesses of the metaphysis and the diaphysis at intervals of 500  $\mu\text{m}$  were  $352.7 \pm 58.6 \mu\text{m}$  (range, 213.6-503.4  $\mu\text{m}$ ) and  $109.3 \pm 3.2 \mu\text{m}$  (range, 81.8-132.6  $\mu\text{m}$ ), respectively (Figure 4, E-H). The histological findings of the AT are shown in Figure 4, I through L. Dense fibrous tissue was observed in the bone-tendon interface in the low-powered HE- and MT-stained images (Figure 4, J-K). The high-powered HE-stained image showed a typical fibrocartilaginous entheses (direct insertion) consisting of the 4 layers of tissue at the bone-tendon interface: AT, uncalcified fibrocartilage, calcified fibrocartilage, and cortical bone (Figure 4L). The mean direct insertion of the AT attached to the distal medial femur from the adductor tubercle toward the distal direction was  $7.9 \pm 1.3 \text{ mm}$  (range, 6.3-9.7 mm).

The periosteal thickness of the metaphysis tended to decrease rapidly at a certain distance from the proximal direction, starting from the medial epicondyle. Six representative examples are shown in Figure 5.

### Radiological Analysis

Four representative examples of radiographs with overlaid graphs of the periosteal thicknesses are shown in Figure 6. In all cases, the thickness of the periosteum changed at the part corresponding to the transition area between diaphyseal and metaphyseal ends of the femur.

### Results of Correlation Analysis

The correlations of cadaveric characteristics and distal femoral dimensions with periosteal thickness at the metaphysis and diaphysis are shown in Table 2. In the region of the metaphysis, periosteal thickness was significantly and positively correlated with female sex ( $r = 0.639$ ), patient height ( $r = 0.703$ ), ML dimension of the femur ( $r = 0.728$ ), AP dimension of the femur ( $r = 0.673$ ), and total length of the femur ( $r = 0.686$ ) ( $P < .01$  for all). In the region of the diaphysis, the thickness of the periosteum was significantly and positively correlated with older age ( $r = 0.738$ ), patient height ( $r = 0.863$ ), ML dimension of the femur ( $r = 0.839$ ), AP dimension of the femur ( $r = 0.781$ ), and total length of the femur ( $r = 0.679$ ) ( $P < .01$  for all).

The direct insertion of the AT was significantly and positively correlated with older age ( $r = 0.758$ ), patient height ( $r = 0.782$ ), ML dimension of the femur ( $r = 0.770$ ), AP dimension of the femur ( $r = 0.704$ ), and total length of the femur ( $r = 0.761$ ) ( $P < .01$  for all) (Table 3).

### DISCUSSION

The most important findings of this study were as follows: (1) the thickness of the periosteum changed at the part corresponding to the transition area between diaphyseal and metaphyseal ends of the femur in all cases, and (2) the direct insertion of the AT was observed up to  $7.9 \pm 1.3 \text{ mm}$  (range, 6.3-9.7 mm) distally, starting from the adductor tubercle.

Based on these findings, we performed biplanar LCWDFO on 2 knees as a pilot test. The osteotomy level was set at the adductor tubercle on the distal medial femur



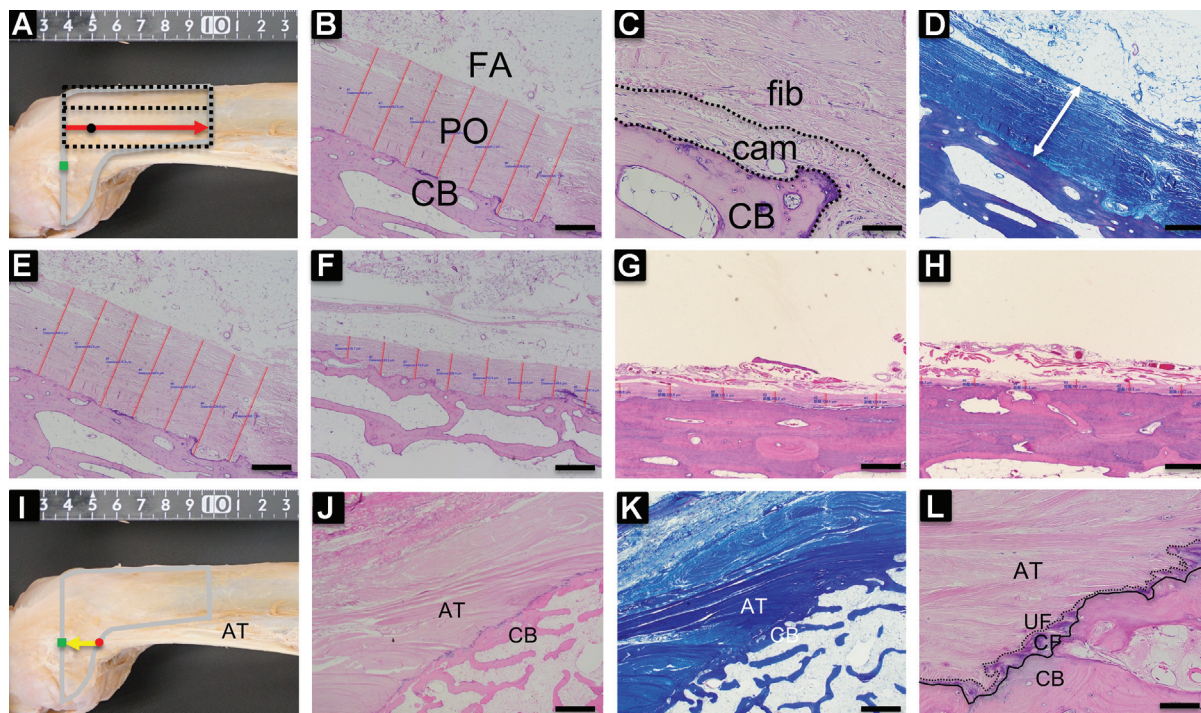


**Figure 4.** Histological examination of the soft tissue around the hinge point for lateral closing-wedge distal femoral osteotomy. The black solid line shows scalebar. (A) The histological section was created as described in Figure 2A. The microscopic findings of the black dot are shown in images B-D. (B) Hematoxylin and eosin (HE) staining ( $\times 4$  magnification; scale bar,  $500\ \mu\text{m}$ ). The low-powered HE-stained image shows a continuous layered structure in contact with the bone cortex. Sparse fibrous adipose tissue is present between the synovial surface of the joint cavity and the periosteum. (C) HE staining ( $\times 40$  magnification; scale bar,  $50\ \mu\text{m}$ ). (D) The layered structure is deeply and equally stained blue by Masson trichrome (white double-headed arrow) ( $\times 4$  magnification; scale bar,  $500\ \mu\text{m}$ ). (E and F) The periosteal thickness in the metaphyseal region on the (E) distal side and (F) proximal side (HE staining;  $\times 4$  magnification; scale bar,  $500\ \mu\text{m}$ ). The periosteum gradually becomes thinner from distal to proximal. (G and H) The periosteal thickness in the diaphyseal region on the (G) distal side and (H) proximal side (HE staining;  $\times 4$  magnification; scale bar,  $500\ \mu\text{m}$ ). The periosteum of the diaphysis is relatively uniform and thin compared with that of the metaphysis. (I) The histological section was created as described in Figure 2C. The microscopic findings of the adductor tubercle (red dot) are shown in images J-L. (J) HE staining ( $\times 4$  magnification; scale bar,  $500\ \mu\text{m}$ ). (K) The adductor tendon is deeply stained blue by Masson trichrome ( $\times 4$  magnification; scale bar,  $500\ \mu\text{m}$ ) (L) HE staining ( $\times 40$  magnification; scale bar,  $50\ \mu\text{m}$ ); black dotted line shows the tidemark. AT, adductor tendon; cam, cambium layer of the periosteum; CB, cortical bone; CF, calcified fibrocartilage; FA, fibrous adipose tissue; fib, fibrous layer of the periosteum; PO, periosteum; UF, uncalcified fibrocartilage.

at which the osteotomy hinge could be fully supported by those soft tissues. Even after the hinge was broken by manual varus-valgus force, the broken hinge was maintained without dislocation by the AT and periosteum (Figure 7 and Supplemental Videos 1 and 2).

These findings suggest that the AT and periosteum support the hinge for LCWDFO within the area surrounded by the upper border of the posterior part of the lateral condyle of the femur and the adductor tubercle; in this region, these soft tissues work as stabilizers, and there is no risk of cutting into the joint space<sup>14</sup> (Figure 8).

In a previous study,<sup>18</sup> we investigated the soft tissue around the hinge point in MCWDFO in 20 fresh-frozen human knees. Dissection of the distal lateral femur revealed the presence of the joint capsule and periosteum around the hinge point, and radiological analysis revealed that the joint capsule is only partially attached to the hinge point in MCWDFO and is fragile enough to be easily

detached during dissection. Histological examination showed sparse fibrous fatty tissue between the synovial surface of the joint cavity and the periosteum; thus, the joint capsule seemed to play a small role in stabilizing the hinge point. In contrast, thick periosteum broadly covered the metaphyseal region, suggesting the supporting role of periosteum against the hinge in MCWDFO.

The present study, which was based on the same method as our previous study,<sup>18</sup> confirmed the presence of the joint capsule, periosteum, and AT around the hinge point for LCWDFO. As in our previous study of the distal lateral femur,<sup>18</sup> the joint capsule was fragile during dissection and the joint capsule had low mechanical strength in the distal medial femur. The mean periosteal thicknesses of the metaphysis and the diaphysis at intervals of  $500\ \mu\text{m}$  were  $352.7 \pm 58.6\ \mu\text{m}$  (range,  $213.6\text{-}503.4\ \mu\text{m}$ ) and  $109.3 \pm 3.2\ \mu\text{m}$  (range,  $81.8\text{-}132.6\ \mu\text{m}$ ), respectively, which were similar to the results of our previous study.<sup>18</sup>

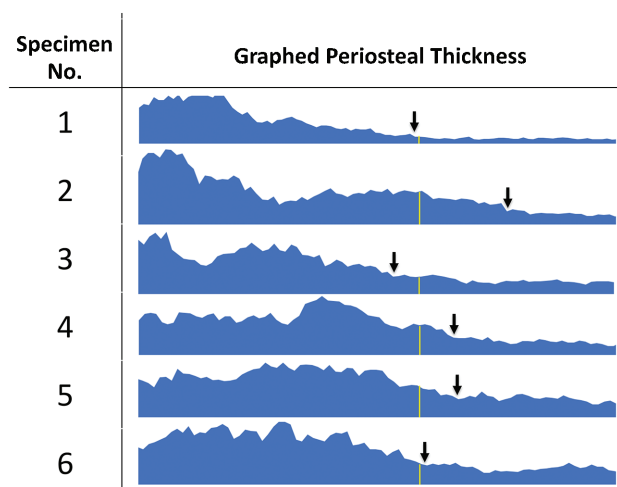


**Figure 5.** Graphed periosteal thickness of the metaphysis in 6 representative samples. The left ends of the graphs represent the medial epicondyle. The yellow line corresponds to 2.5 cm, which is equal to the diameter of the calibrator used to overlay the graphs for radiological analysis. The periosteal thickness tended to decrease rapidly at a certain distance from the lateral epicondyle (black arrows).

In the previous study, the thickness of the periosteum correlated with age, sex, ML and AP dimensions of the femur, total length of the femur, and height, reflecting aging, changing serum estrogen concentrations, and mechanical stress.<sup>18</sup> Furthermore, radiological analysis with image editing software revealed a tendency for the thickness of the periosteum to change at the part corresponding to the transition area between diaphyseal and metaphyseal ends of the femur in all cases analyzed in the present study; this was also observed in the previous study of the distal lateral femur.<sup>18</sup> The present study also revealed the presence of the AT on the distal medial femur, showing that the soft tissues supporting the hinge point in the distal medial femur differ to those on the distal lateral femur.

In a retrospective radiographic study of 100 patients who underwent lateral open wedge distal femoral osteotomy, Winkler et al<sup>24</sup> reported that the incidence of hinge fractures of the medial bone cortex was significantly higher when the hinge was created proximal to the adductor tuberosity compared with distally (53% vs 27%). The authors concluded that surgeons should aim to position the osteotomy hinge at the level of or distal to the proximal margin of the adductor tubercle to minimize the risk of medial cortical hinge fracture.<sup>24</sup> Using a similar method, Rupp et al<sup>20</sup> investigated 79 radiographs after LCWDFO

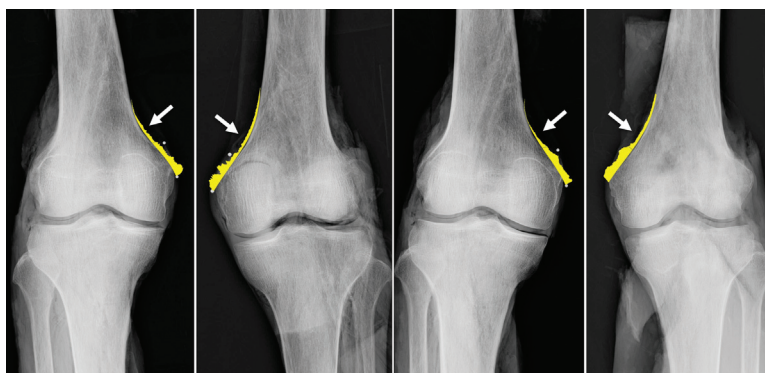


**Figure 6.** Representative examples of radiographs with overlaid graphs of periosteal thicknesses (shaded in yellow). In all cases, the thickness overlaid graphs of periosteal of the periosteum changed at the part corresponding to the apex of the turning point of the metaphysis of the femur (white arrows).

**TABLE 2**  
Correlations of Cadaveric Characteristics and Distal Femoral Dimensions  
With Periosteal Thickness at the Metaphysis and Diaphysis<sup>a</sup>

Characteristic	Periosteal Thickness at the Metaphysis		Periosteal Thickness at the Diaphysis	
	<i>r</i>	<i>P</i>	<i>r</i>	<i>P</i>
Older age	0.504	.17	0.738	<.01
Female sex	0.639	<.01	0.058	.807
Height	0.703	<.01	0.863	<.01
Femur, mediolateral	0.728	<.01	0.839	<.01
Femur, anteroposterior	0.673	<.01	0.781	<.01
Femur, length	0.686	<.01	0.679	<.01

<sup>a</sup>Boldface *P* values indicate statistical significance ( $P < .05$ ).



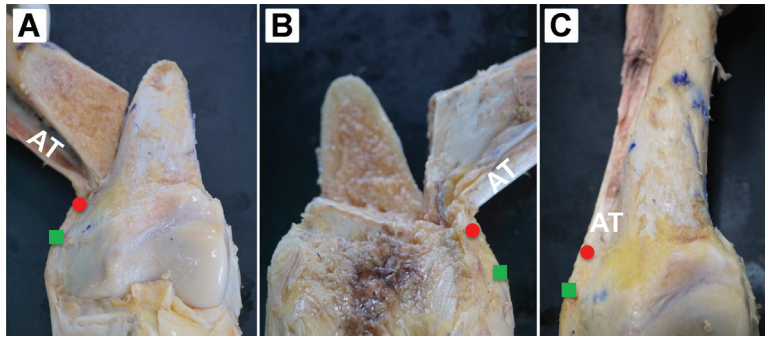


**Figure 7.** Biplanar lateral closing-wedge distal femoral osteotomy as a pilot test: (A) anteroposterior view, (B) posteroanterior view, and (C) anteroposterior view of the broken hinge. (A and B) The hinge is manually broken with varus-valgus force (see Supplemental Video 1). (C) The broken hinge is maintained without dislocation by the adductor tendon (AT) and periosteum (see Supplemental Video 2). Red circle, adductor tubercle; green square, medial epicondyle of the femur.

**TABLE 3**  
Correlations of Cadaveric Characteristics and Distal Femoral Dimensions With Direct Insertion of the Adductor Tendon<sup>a</sup>

Characteristic	Direct Insertion of the AT	
	<i>r</i>	<i>P</i>
Older age	0.758	<.01
Female sex	0.287	.22
Height	0.782	<.01
Femur, mediolateral	0.770	<.01
Femur, anteroposterior	0.704	<.01
Femur, length	0.761	<.01

<sup>a</sup>Boldface *P* values indicate statistical significance (*P* < .05). AT, adductor tendon.

and evaluated the incidence of hinge fractures by characteristics of the osteotomy site, namely the length and inclination of the osteotomy, horizontal distance between the medial cortical bone and osteotomy hinge, and vertical distance between the osteotomy hinge and proximal border of the AT. The incidence of medial cortical hinge fracture was 48% (extension fracture type [68%], followed by proximal [21%] and distal [11%] fracture types), and the incidence of malunion after hinge fracture was 14%. Rupp et al concluded that the risk of hinge fracture increases with increasing osteotomy wedge height and a hinge position close to the medial cortex and that dislocation of a medial hinge fracture by >2 mm is associated with malunion. In contrast, neither the craniocaudal position of the hinge relative to the AT nor the ML distance between the hinge and the AT significantly influenced the incidence of medial cortical hinge fracture.<sup>20</sup>

These 2 studies<sup>20,24</sup> reported conflicting results regarding the incidence of medial cortical hinge fracture based on the positional relationship between the adductor tubercle and the hinge position. Moreover, the relationship between the hinge point and fracture morphology and the amount of dislocation have not been fully investigated. Although

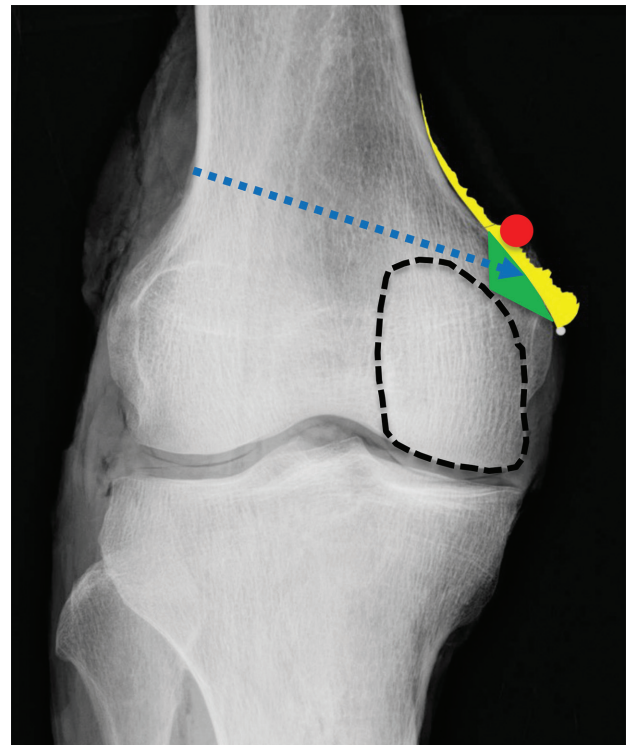


**Figure 8.** Area supported by the adductor muscle tendon and periosteum in lateral closing-wedge distal femoral osteotomy (shaded in green). Red circle, adductor tubercle; dashed black area, posterior part of the lateral condyle; blue dotted arrow, distal cut in lateral closing-wedge distal femoral osteotomy; yellow-shaded area, graphical representation of periosteal thickness.

these 2 studies suggested that the soft tissue plays a role in stabilizing the hinge point in the distal medial femur,<sup>20,24</sup> this role remains unclear. The present study revealed the presence of the joint capsule, AT, and periosteum as soft tissue in the distal medial femur and showed the area supported by these soft tissue structures for

LCWDFO, which may lead to further research to investigate the mechanical strength of these soft tissues in stabilizing the hinge point. It has also been reported that bone density affects elasticity and stiffness, which correlate with the occurrence of hinge fractures<sup>3,7,10</sup>; thus, further multifaceted evaluation is needed to determine the specific safe zone for the hinge point for LCWDFO.

The present study revealed that the AT had direct insertion that was present up to  $7.9 \pm 1.3$  mm (range, 6.3-9.7 mm) distally, starting from the adductor tubercle. Furthermore, the measured calcified fibrocartilage layer was significantly correlated with older age ( $r = 0.758$ ;  $P < .01$ ), which was consistent with findings of a previous study reporting that the aged shoulder rotator cuff enthesis is typified by an increased calcified zone.<sup>12</sup>

### Limitations

The present study has some limitations. First, the mean age of the cadavers was  $82.7 \pm 7.8$  years (range, 60-96 years), which is older than most patients undergoing LCWDFO. Nevertheless, age seemed to have little influence on the morphological features of the turning point of the periosteal thickness and the anatomic location of the AT attachment. Second, the present study used cadavers fixed with formalin. Although the joint capsule was fragile enough to be easily detached during dissection, changes in mechanical properties caused by tissue fixation were not considered. Third, the mechanical strengths of the periosteum and AT were not evaluated. Nevertheless, this is the first study to report quantitative measurements of the thickness of the periosteum and direct insertion of the AT around the hinge point for LCWDFO.

### CONCLUSION

The study findings indicated that the periosteum and AT support the hinge for LCWDFO within the area surrounded by the apex of the adductor tubercle and the upper border of the posterior part of the lateral femoral condyle.

### ACKNOWLEDGMENTS

The authors express their sincere gratitude to all the patients and their families who agreed to the donation of the bodies used in this research. The authors also thank Tadahisa Uemura, the chief engineer of our institute, for helping with the radiological study, and Kelly Zammit, from Edanz (<https://jp.edanzgroup.com/ac>), for editing a draft of the article.

### REFERENCES

1. Akamatsu Y, Kumagai K, Kobayashi H, Tsuji M, Saito T. Effect of increased coronal inclination of the tibial plateau after opening-wedge high tibial osteotomy. *Arthroscopy*. 2018;34(7):2158-2169.
2. Babis GC, An KN, Chao EY, Rand JA, Sim FH. Double level osteotomy of the knee: a method to retain joint-line obliquity: clinical results. *J Bone Joint Surg Am*. 2002;84(8):1380-1388.
3. Bayraktar HH, Morgan EF, Niebur GL, Morris GE, Wong EK, Keaveny TM. Comparison of the elastic and yield properties of human femoral trabecular and cortical bone tissue. *J Biomech*. 2004;37(1):27-35.
4. Benjamin M, Kumai T, Milz S, et al. The skeletal attachment of tendons—tendon “entheses.” *Comp Biochem Physiol A Mol Integr Physiol*. 2002;133(4):931-945.
5. Benjamin M, Toumi H, Ralphs JR, et al. Where tendons and ligaments meet bone: attachment sites (“entheses”) in relation to exercise and/or mechanical load. *J Anat*. 2006;208(4):471-490.
6. Han SB, Lee DH, Shetty GM, et al. A “safe zone” in medial opening-wedge high tibia osteotomy to prevent lateral cortex fracture. *Knee Surg Sports Traumatol Arthrosc*. 2013;21(1):90-95.
7. Hart NH, Nimphius S, Rantalainen T, Ireland A, Siafarikas A, Newton RU. Mechanical basis of bone strength: influence of bone material, bone structure and muscle action. *J Musculoskelet Neuronal Interact*. 2017;17(3):114-139.
8. Kim TW, Lee MC, Cho JH, Kim JS, Lee YS. The ideal location of the lateral hinge in medial closing wedge osteotomy of the distal femur: analysis of soft tissue coverage and bone density. *Am J Sports Med*. 2019;47(12):2945-2951.
9. Kinoshita T, Hashimoto Y, Iida K, Nakamura H. ACL graft matching: cadaveric comparison of microscopic anatomy of quadriceps and patellar tendon grafts and the femoral ACL insertion site. *Am J Sports Med*. 2022;50(11):2953-2960.
10. Lee YS, Won JS, Oh WS, Park HG, Lee BK. Lateral tibial bone mineral density around the level of the proximal tibiofibular joint. *Knee Surg Sports Traumatol Arthrosc*. 2014;22(7):1678-1683.
11. Lobenhoffer P, Agneskirchner JD. Improvements in surgical technique of valgus high tibial osteotomy. *Knee Surg Sports Traumatol Arthrosc*. 2003;11(3):132-138.
12. Long Z, Nakagawa K, Wang Z, et al. Age-related cellular and microstructural changes in the rotator cuff enthesis. *J Orthop Res*. 2022;40(8):1883-1895.
13. Miller BS, Dorsey WO, Bryant CR, Austin JC. The effect of lateral cortex disruption and repair on the stability of the medial opening wedge high tibial osteotomy. *Am J Sports Med*. 2005;33(10):1552-1557.
14. Nakamura R, Akiyama T, Takeuchi R, Nakayama H, Kondo E. Medial closed wedge distal femoral osteotomy using a novel plate with an optimal compression system. *Arthrosc Tech*. 2021;10(6):e1497-e1504.
15. Nakamura R, Komatsu N, Fujita K, et al. Appropriate hinge position for prevention of unstable lateral hinge fracture in open wedge high tibial osteotomy. *Bone Joint J*. 2017;99-B(10):1313-1318.
16. Nakayama H, Schröter S, Yamamoto C, et al. Large correction in opening wedge high tibial osteotomy with resultant joint-line obliquity induces excessive shear stress on the articular cartilage. *Knee Surg Sports Traumatol Arthrosc*. 2018;26(6):1873-1878.
17. Nasu H, Nimura A, Sugiura S, et al. An anatomic study on the attachment of the joint capsule to the tibia in the lateral side of the knee. *Surg Radiol Anat*. 2018;40(5):499-506.
18. Oda T, Maeyama A, Yoshimura I, et al. Soft tissue stabilization of the hinge position in medial closed wedge distal femoral osteotomy: an anatomical study. *BMC Musculoskelet Disord*. 2022;23(1):1105.
19. Plank J, Rychlo A. A method for quick decalcification. *Zentralbl Allg Pathol*. 1952;89(8):252-254.
20. Rupp MC, Winkler PW, Lutz PM, et al. Dislocated hinge fractures are associated with malunion after lateral closing wedge distal femoral osteotomy. *Knee Surg Sports Traumatol Arthrosc*. 2022;30(3):982-992.
21. Schröter S, Nakayama H, Yoshiya S, et al. Development of the double level osteotomy in severe varus osteoarthritis showed good

A Video Supplement for this article is available at <https://journals.sagepub.com/doi/full/10.1177/23259671241233014#supplementary-materials>.



- outcome by preventing oblique joint line. *Arch Orthop Trauma Surg.* 2019;139(4):519-627.
22. Schuster P, Geßlein M, Schlumberger M, et al. Ten-year results of medial open-wedge high tibial osteotomy and chondral resurfacing in severe medial osteoarthritis and varus malalignment. *Am J Sports Med.* 2018;46(6):1362-1370.
  23. Staubli AE, De Simoni C, Babst R, Lobenhoffer P. TomoFix: a new LCP-concept for open wedge osteotomy of the medial proximal tibia—early results in 92 cases. *Injury.* 2003;34(suppl 2):B55-B62.
  24. Winkler PW, Rupp MC, Lutz PM, et al. A hinge position distal to the adductor tubercle minimizes the risk of hinge fractures in lateral open wedge distal femoral osteotomy. *Knee Surg Sports Traumatol Arthrosc.* 2021;29(10):3382-3391.